What'sNew in the New Build 10 OCO-2/3 SIF Lite Data Products

slack channel: iposter_Kurosu_SIF

T P Kurosu1, C.Frankenberg2, P. Köhler2, P. Somkuti3, N. Parazoo1, A. Eldering1

1Jet Propulsion Lab/California Institute of Technology3California Instituteof Technology2Colorado State University

PRESENTED AT:

SUMMARY

The Build 10 solar induced fluorescence (SIF) OCO-2&3 Lite product contains a subset of the information in the IMAP-DOAS (IDP) pre-processing L2 files. There is one file per day, for each day that has had at least one successfully retrieved sounding. The main purpose of the SIF Lite product is to perform post-processing on the original IDP files and to provide all valid data in significantly smaller files that still contain all necessary information for typical science analyses. SIF Lite data have the some added value compared to the original IDP retrievals:

- Only converged soundings that passed initial quality criteria thresholds are included
- Application of an important SIF offset-correction procedure, performed on a daily basis using non-fluorescing surfaces such as deserts or most oceans
- Additional information merged from both the A Band preprocessor (ABP) as well as meteorological input data interpolated to the OCO-2&3 footprint in time and space.

The SIF-lite files are provided in netCDF-4 format, a self-documenting data format that allows for the organization of the data file into Dimensions, Groups, Variables, and Attributes. Variable Attributes provide descriptive information about each data field, including units, scale_factor, add_offset, and description.

The Early Version of the SIF Lite product has been publicly released, and data are available at the GES DISC (https://disc.gsfc.nasa.gov/datasets/OCO3_L2_Lite_SIF_EarlyR/summary?keywords=OCO3_L2_Lite_SIF_EarlyR). An updated README file has just been released and should be consulted for product details and file organization.

MAJOR PRODUCT UPDATES

Several updates have been made to the Build 10 SIF Lite product. The main ones are listed here. For details, please consult the product README file distributed with the data.

Data Selection

The selection of SIF soundings has changed in the current B10 version: while previously SIF data were already filtered according to basic quality criteria, the B10 SIF Lite files now include all soundings for which the standard L2 data field sounding_qual_flag = 0. This leads to an increase in data volume, and it also makes it necessary to filter data according to the new Quality_Flag field

The Quality Flag

New in SIF Lite B10 is the Quality_Flag variable that indicates the data quality level for each sounding in the OCO-2&3 SIF Lite file. Quality_Flag is set to one of three values: best (0), good (1), and failed (2). For science studies it is recommended to use the combined soundings of best&good. The criteria used to assign the quality flag are a combination of absolute radiance values, retrieval χ^2, O_2 and CO_2 ratios, solar zenith angle, and land cover fraction in the ground pixel.

Improved Bias/Offset Correction

The main retrieval quantity in the IMAP DOAS product is relative fluorescence [Frankenberg *et al.* (2011a,b)]., *i.e.*, the fractional contribution of SIF to the continuum level radiance. Absolute SIF is being generated in the SIF Lite post-processing step. Owing to various effects like uncertainties in the exact instrument line-shape per footprint or slight uncertainties in detector linearity, biases in retrieved SIF can occur and need to be corrected.

The bias/offset correction requires determination of the background signal over non-fluorescing ("barren") surfaces, which is then subtracted from all SIF values. For B10, the identification of barren surfaces is based on a combination of the 2018 MODIS IGBP barren/snow land classification and Vegetation Photosynthesis Model (VPM) GPP ≈ 0 [Zhang *et al.*, 2017], which have been compiled into an external data base tabulated on a global grid with 0.2°×0.2° resolution. The background signal is calculated from the average of SIF over barren surfaces from three days of observation (current ±1 day).

SIF at 740 nm

Satellite-based estimates of SIF are typically reported at a reference wavelength of 740 nm for moderate spectral resolution and at 757 or 771 nm for high spectral resolution sensors [*c.f.*, Parazoo *et al*., 2019]. This may confound inter-sensor comparisons. 740 nm is used because it is near the peak of the SIF emission feature in the far-red, while 757 or 771 nm as a reference wavelength for OCO-2/3 and GOSAT is driven by the ability to perform narrow band retrievals and the lack of larger spectral regions capable of performing SIF retrievals. Although the inter-sensor wavelength range is relatively small, absolute fluorescence values vary greatly in this region [Joiner *et al.*, 2013; Köhler *et al.*, 2018; Sun *et al*., 2018]. Reference SIF shapes derived from leaf-level studies suggest that far-red fluorescence spectra, and thus wavelength conversions, are roughly consistent across species [Magney *et al*., 2019].

In the OCO-2/3 B10 SIF Lite data product, the actual SIF retrievals are performed at 757 and 771 nm, and SIF at 740 nm is derived from these two values based on the following relationship:

$$\mathbf{SIF@740nm = 1.5 \cdot (SIF@757nm + 2 \cdot SIF@771nm) / 2}$$

Product File Structure

Users of previous OCO-2 SIF Lite files (prior to Build 10) will find that the file organization has changed significantly: in addition to a set of main variables in the root group of the file, the structure of each SIF Lite file includes Dimensions, Global Attributes, and auxiliary data organized in the groups Cloud, Geolocation, Metadata, Meteo, Offset, and Science. Variables of prime interest are collected in the root group ("/") of the file, and some of these are duplicated in the subgroups. The image below show a partial view of a product data file using the Panoply Data Viewer (http://www.giss.nasa.gov/tools/panoply).

It should be noted at this point that all meteorological fields in the Meteo group are taken from GEOS-5 FP-IT forecasts, and that they are provided “as is”, *i.e.*, not fully validated.

A final note: SIF Lite files for OCO-2 and OCO-3 files have identical file structures, with information on the observing sensor provided in the (Global) Attributes. Furthermore, offset adjustment and quality flag assignment are performed in exactly the same way for both sensors.

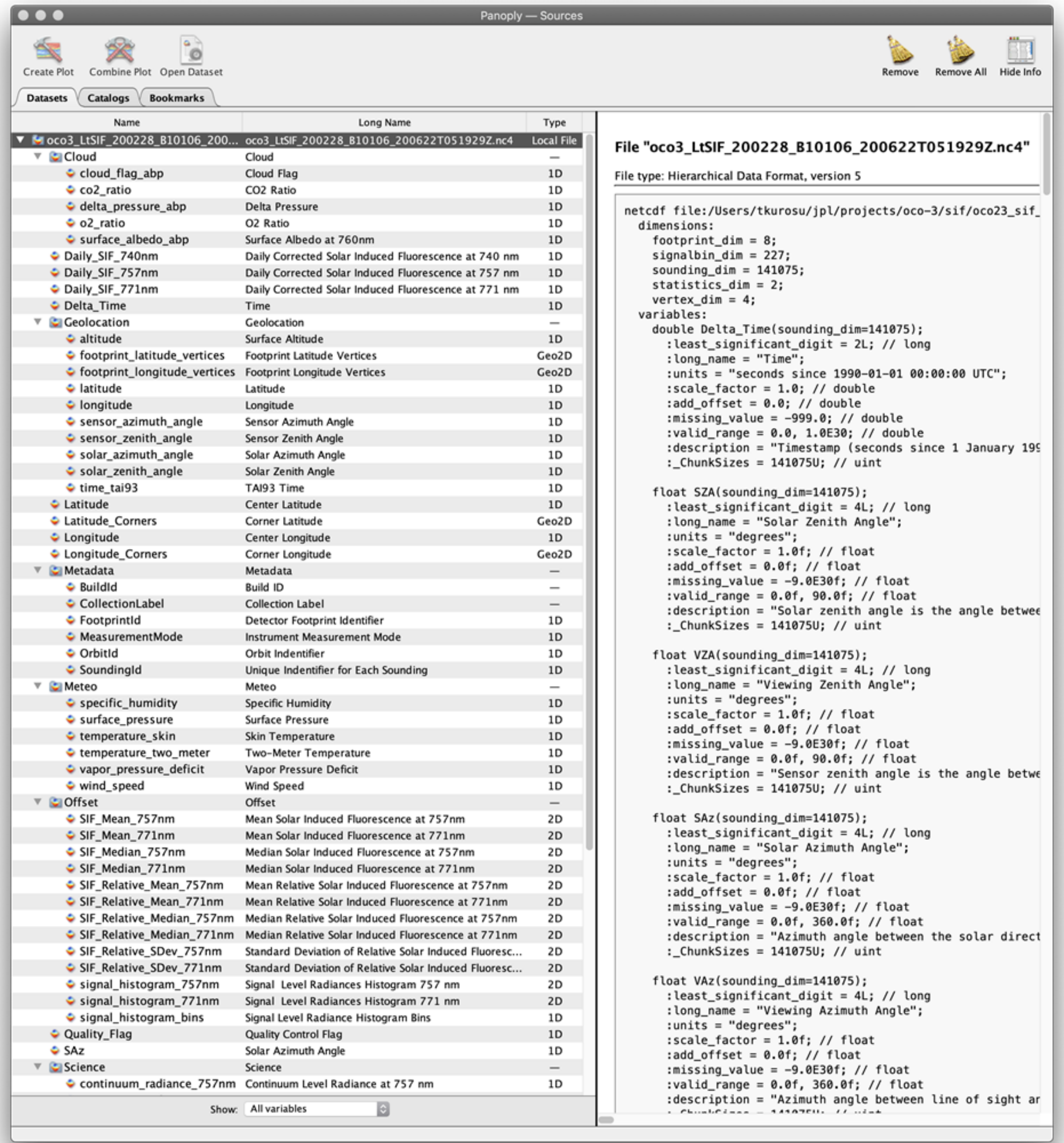
Panoply — Sources
Create Plot
Combine Plot
Open Dataset
Remove
Remove All
Hide Info
Datasets
Catalogs
Bookmarks
Name
Long Name
Type
oco3_LtSIF_200228_B10106_200... oco3_LtSIF_200228_B10106_200622T051929Z.nc4 Local File
Cloud Cloud —
cloud_flag_abp Cloud Flag 1D
co2_ratio CO2 Ratio 1D
delta_pressure_abp Delta Pressure 1D
o2_ratio O2 Ratio 1D
surface_albedo_abp Surface Albedo at 760nm 1D
Daily_SIF_740nm Daily Corrected Solar Induced Fluorescence at 740 nm 1D
Daily_SIF_757nm Daily Corrected Solar Induced Fluorescence at 757 nm 1D
Daily_SIF_771nm Daily Corrected Solar Induced Fluorescence at 771 nm 1D
Delta_Time Time 1D
Geolocation Geolocation —
altitude Surface Altitude 1D
footprint_latitude_vertices Footprint Latitude Vertices Geo2D
footprint_longitude_vertices Footprint Longitude Vertices Geo2D
latitude Latitude 1D
longitude Longitude 1D
sensor_azimuth_angle Sensor Azimuth Angle 1D
sensor_zenith_angle Sensor Zenith Angle 1D
solar_azimuth_angle Solar Azimuth Angle 1D
solar_zenith_angle Solar Zenith Angle 1D
time_tai93 TAI93 Time 1D
Latitude Center Latitude 1D
Latitude_Corners Corner Latitude Geo2D
Longitude Center Longitude 1D
Longitude_Corners Corner Longitude Geo2D
Metadata Metadata —
BuildId Build ID —
CollectionLabel Collection Label —
FootprintId Detector Footprint Identifier 1D
MeasurementMode Instrument Measurement Mode 1D
OrbitId Orbit Indentifier 1D
SoundingId Unique Indentifier for Each Sounding 1D
Meteo Meteo —
specific_humidity Specific Humidity 1D
surface_pressure Surface Pressure 1D
temperature_skin Skin Temperature 1D
temperature_two_meter Two-Meter Temperature 1D
vapor_pressure_deficit Vapor Pressure Deficit 1D
wind_speed Wind Speed 1D
Offset Offset —
SIF_Mean_757nm Mean Solar Induced Fluorescence at 757nm 2D
SIF_Mean_771nm Mean Solar Induced Fluorescence at 771nm 2D
SIF_Median_757nm Median Solar Induced Fluorescence at 757nm 2D
SIF_Median_771nm Median Solar Induced Fluorescence at 771nm 2D
SIF_Relative_Mean_757nm Mean Relative Solar Induced Fluorescence at 757nm 2D
SIF_Relative_Mean_771nm Mean Relative Solar Induced Fluorescence at 771nm 2D
SIF_Relative_Median_757nm Median Relative Solar Induced Fluorescence at 757nm 2D
SIF_Relative_Median_771nm Median Relative Solar Induced Fluorescence at 771nm 2D
SIF_Relative_SDev_757nm Standard Deviation of Relative Solar Induced Fluoresc... 2D
SIF_Relative_SDev_771nm Standard Deviation of Relative Solar Induced Fluoresc... 2D
signal_histogram_757nm Signal Level Radiances Histogram 757 nm 2D
signal_histogram_771nm Signal Level Radiances Histogram 771 nm 2D
signal_histogram_bins Signal Level Radiance Histogram Bins 1D
Quality_Flag Quality Control Flag 1D
SAz Solar Azimuth Angle 1D
Science Science —
continuum_radiance_757nm Continuum Level Radiance at 757 nm 1D
Show: All variables
File "oco3_LtSIF_200228_B10106_200622T051929Z.nc4"
File type: Hierarchical Data Format, version 5
netcdf file:/Users/tkurosu/jpl/projects/oco-3/sif/oco23_sif_
dimensions:
footprint_dim = 8;
signalbin_dim = 227;
sounding_dim = 141075;
statistics_dim = 2;
vertex_dim = 4;
variables:
double Delta_Time(sounding_dim=141075);
:least_significant_digit = 2L; // long
:long_name = "Time";
:units = "seconds since 1990-01-01 00:00:00 UTC";
:scale_factor = 1.0; // double
:add_offset = 0.0; // double
:missing_value = -999.0; // double
:valid_range = 0.0, 1.0E30; // double
:description = "Timestamp (seconds since 1 January 19
:_ChunkSizes = 141075U; // uint
float SZA(sounding_dim=141075);
:least_significant_digit = 4L; // long
:long_name = "Solar Zenith Angle";
:units = "degrees";
:scale_factor = 1.0f; // float
:add_offset = 0.0f; // float
:missing_value = -9.0E30f; // float
:valid_range = 0.0f, 90.0f; // float
:description = "Solar zenith angle is the angle betwe
:_ChunkSizes = 141075U; // uint
float VZA(sounding_dim=141075);
:least_significant_digit = 4L; // long
:long_name = "Viewing Zenith Angle";
:units = "degrees";
:scale_factor = 1.0f; // float
:add_offset = 0.0f; // float
:missing_value = -9.0E30f; // float
:valid_range = 0.0f, 90.0f; // float
:description = "Sensor zenith angle is the angle betwe
:_ChunkSizes = 141075U; // uint
float SAz(sounding_dim=141075);
:least_significant_digit = 4L; // long
:long_name = "Solar Azimuth Angle";
:units = "degrees";
:scale_factor = 1.0f; // float
:add_offset = 0.0f; // float
:missing_value = -9.0E30f; // float
:valid_range = 0.0f, 360.0f; // float
:description = "Azimuth angle between the solar direct
:_ChunkSizes = 141075U; // uint
float VAz(sounding_dim=141075);
:least_significant_digit = 4L; // long
:long_name = "Viewing Azimuth Angle";
:units = "degrees";
:scale_factor = 1.0f; // float
:add_offset = 0.0f; // float
:missing_value = -9.0E30f; // float
:valid_range = 0.0f, 360.0f; // float
:description = "Azimuth angle between line of sight ar

OCO-2/3 COMPARISON

The global images of monthly average SIF Lite in the slide sorter below appear to indicate that the global SIF distributions observed by OCO-2 and OCO-3 products are quite similar. However, more than a "χ-by-eye" is required to assess the similarity of the two data products. SIF has a strong diurnal dependence, so the difference in observation times - OCO-2 observes at more or less the same local solar time at any given latitude, while OCO-3 records SIF between sun-up and sun-down - are expected to manifest in observed SIF. On the other hand, it is exactly this diurnal variation that the application of the Daily Correction Factor is supposed to equalize.

Below are four images with histograms of OCO-2 and OCO-3 Daily SIF at 740 nm, compiled from 0.2°×0.2° seasonal averages (DJF, MAM, JJA, SON) over the OCO-3 data record. Only grid boxes where both sensors have made observations are included in the histograms. Each plot contains a legend with the global mean and standard deviation of the SIF observations from each instrument. As is apparent from the histograms, OCO-2 and OCO-3 do indeed observe a similar distribution SIF across the globe. While OCO-3 SIF appears to be shifted to overall smaller absolute values, the near-identical shapes of the curves indicate that the SIF Lite products from OCO-2 and OCO-3 are consistent. A more thorough analysis of the data product has yet to be performed.

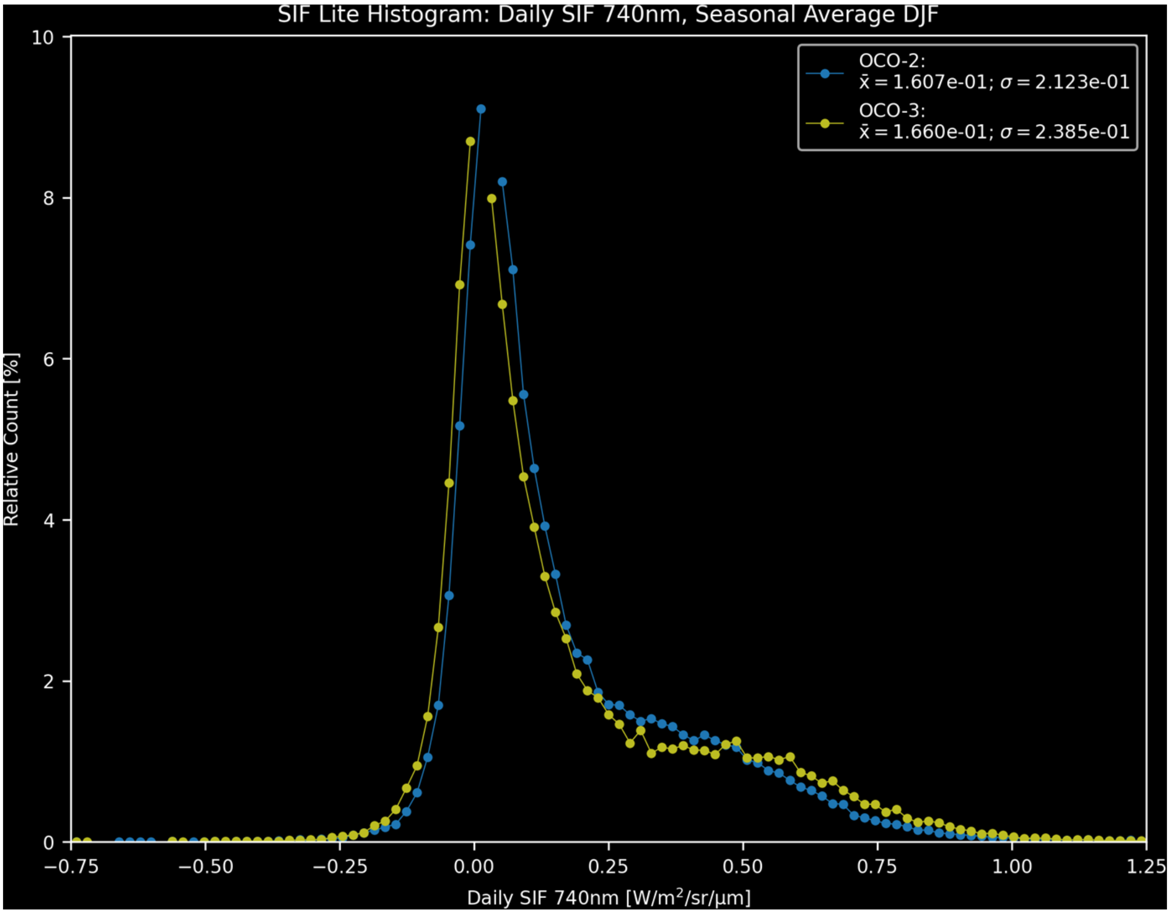

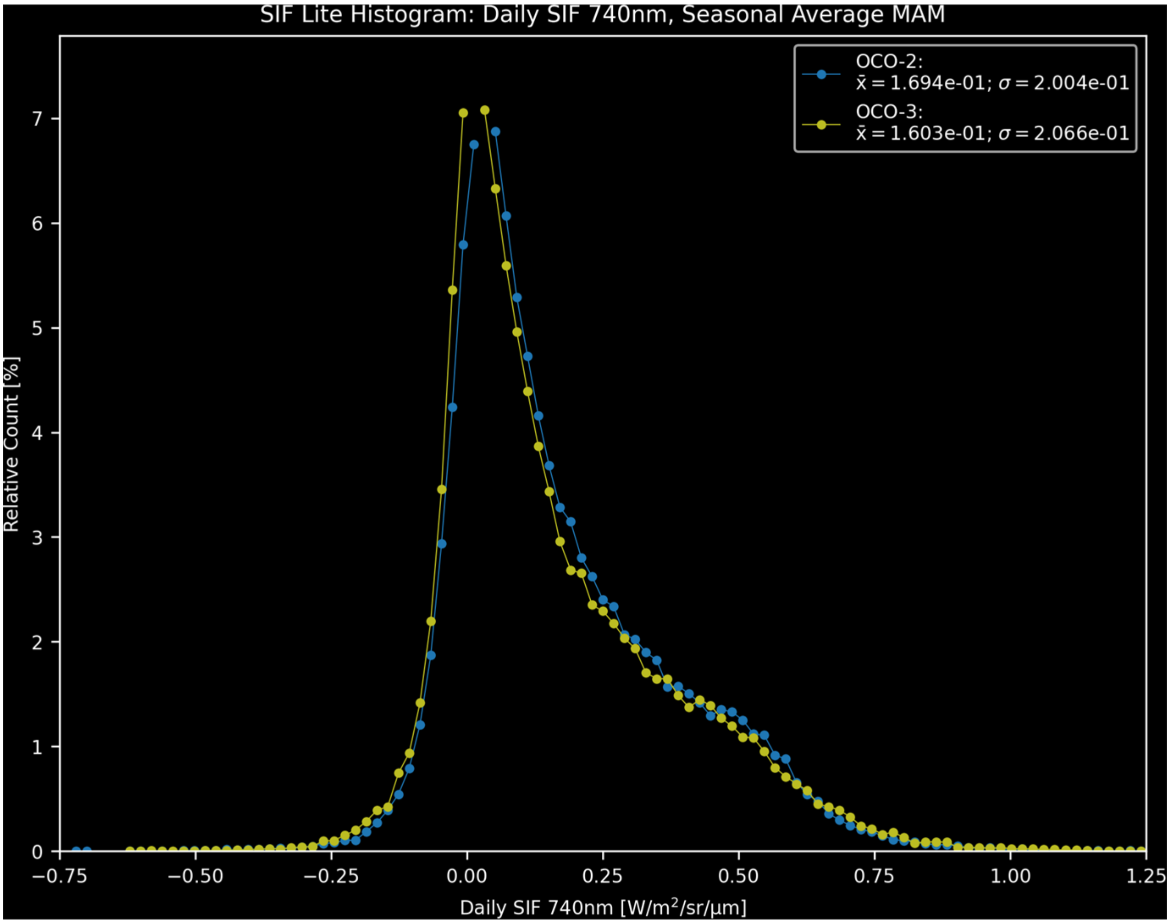
SIF Lite Histogram: Daily SIF 740nm, Seasonal Average MAM
OCO-2:
x̄ = 1.694e-01; σ = 2.004e-01
OCO-3:
x̄ = 1.603e-01; σ = 2.066e-01
Relative Count [%]
Daily SIF 740nm [W/m2/sr/µm]

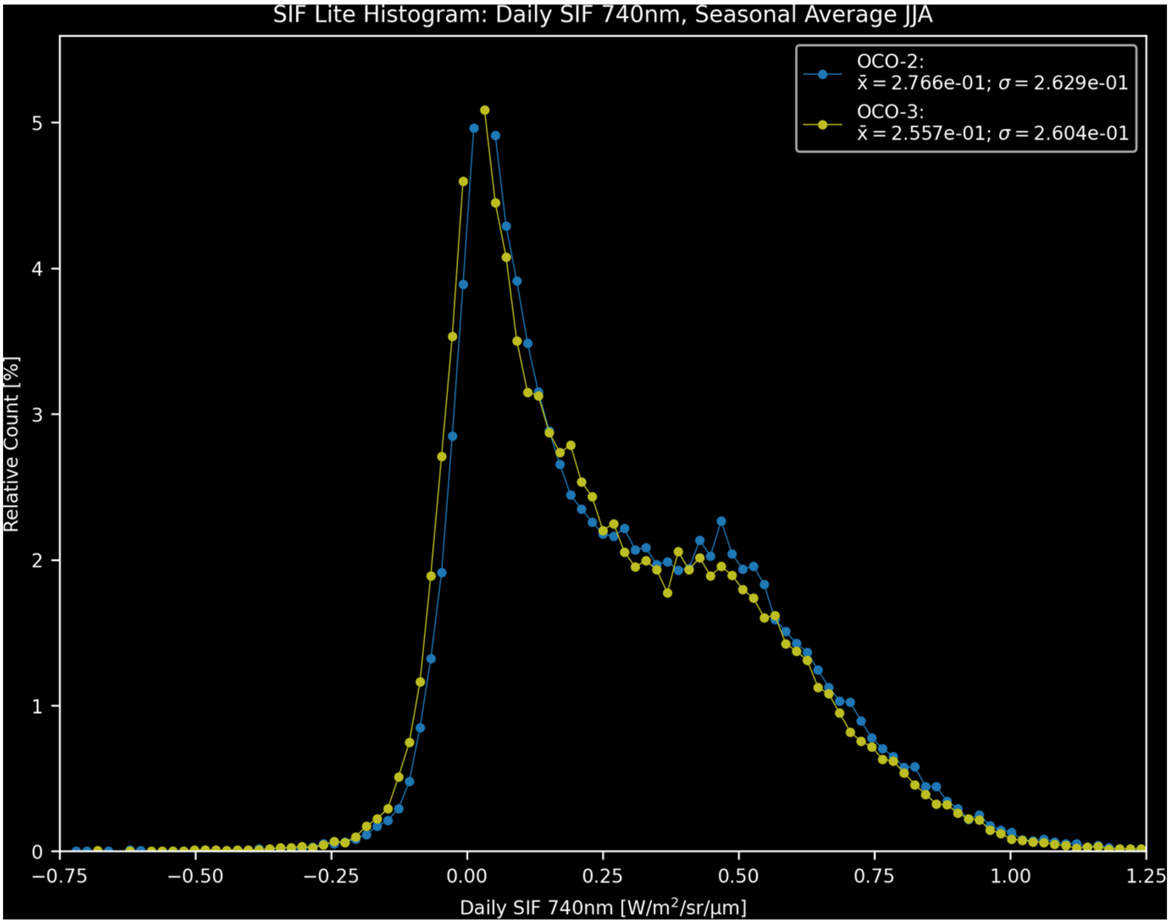
SIF Lite Histogram: Daily SIF 740nm, Seasonal Average JJA
OCO-2:
x̄ = 2.766e-01; σ = 2.629e-01
OCO-3:
x̄ = 2.557e-01; σ = 2.604e-01
Relative Count [%]
Daily SIF 740nm [W/m2/sr/µm]

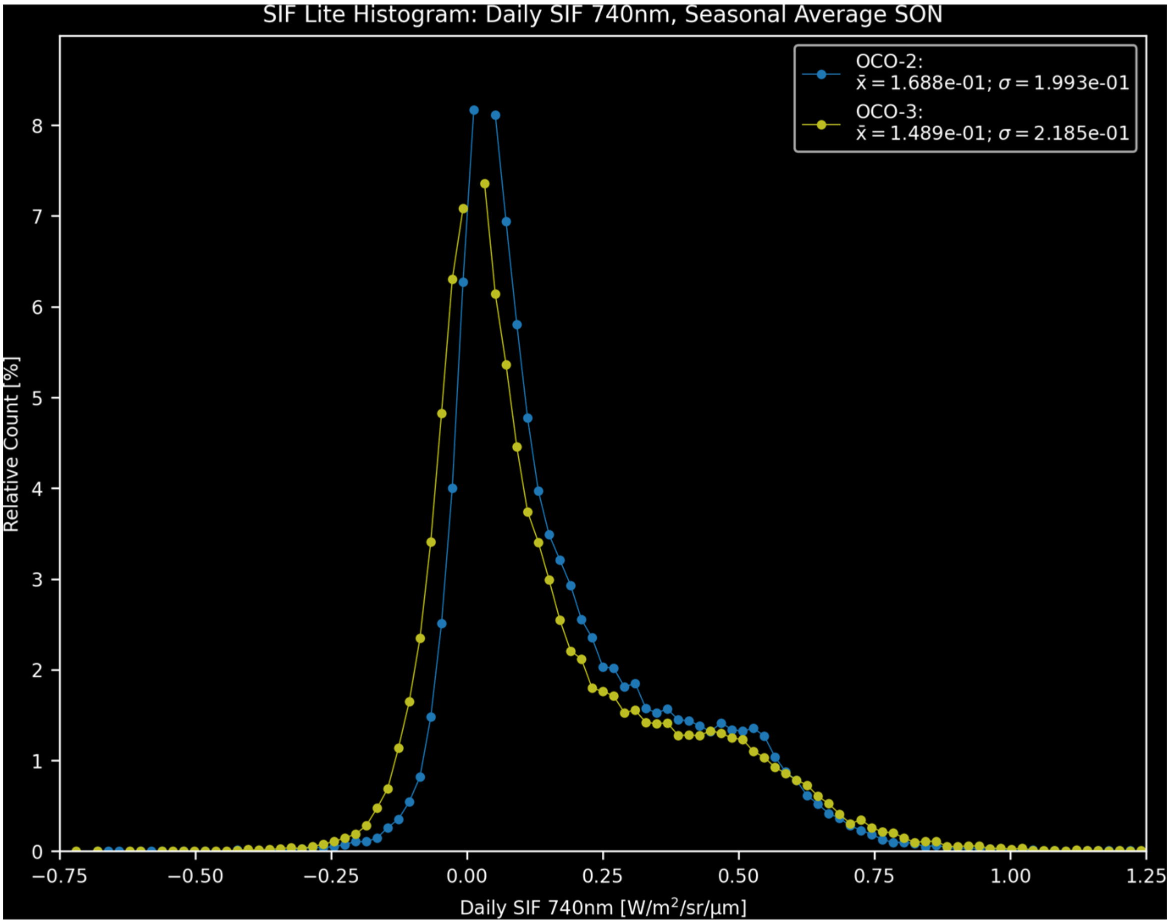
SIF Lite Histogram: Daily SIF 740nm, Seasonal Average SON
OCO-2:
x̄ = 1.688e-01; σ = 1.993e-01
OCO-3:
x̄ = 1.489e-01; σ = 2.185e-01
Relative Count [%]
Daily SIF 740nm [W/m2/sr/μm]
0
1
2
3
4
5
6
7
8
−0.75
−0.50
−0.25
0.00
0.25
0.50
0.75
1.00
1.25

WHAT ABOUT GOSAT?

In the course of updating the OCO-2&3 Build 10 SIF Lite products, it was decided to carry over the OCO updates to ACOS/GOSAT Build 9. While an ACOS Build 10 is as yet pending, the latest ACOS/GOSAT SIF Lite product includes all the updates of the OCO-2&3 SIF Lite data products (see "Major Product Updates" box). This includes the selection of data for post-processing, the new Quality Flag, improved bias/offset correction, SIF at 740 nm, and an updated file structure similar to that of OCO-2&3.

ACOS/GOSAT B9 SIF Lite differs from OCO-2&3 B10 SIF Lite in the following ways:

- Criteria for sounding selection are slightly relaxed, accepting solar zenith angles up to 80° as "good" (compared to 70° for OCO-2&3), to allow more data at higher latitudes in the sparse GOSAT record.
- Offset/bias correction is derived from observations with a ±15 day time window around the day to be corrected (±1 day for OCO-2&3).
- File structure and product dimension account for the fact that GOSAT observes S&P polarization components separately, resulting in an extra dimension of some of the SIF product variables.

The images below show 2019 seasonal averages (DJF, MAM, JJA, SON) of ACOS/GOSAT S-Polarization Daily SIF at 740 nm. Due to the sparseness of the GOSAT spatial coverage, the data have been gridded to 0.5°×0.5° for enhanced visibility.

NOTE: the images below are based on temporary, off-line processed ACOS/GOSAT SIF Lite data. The official data product will become available in the near future.

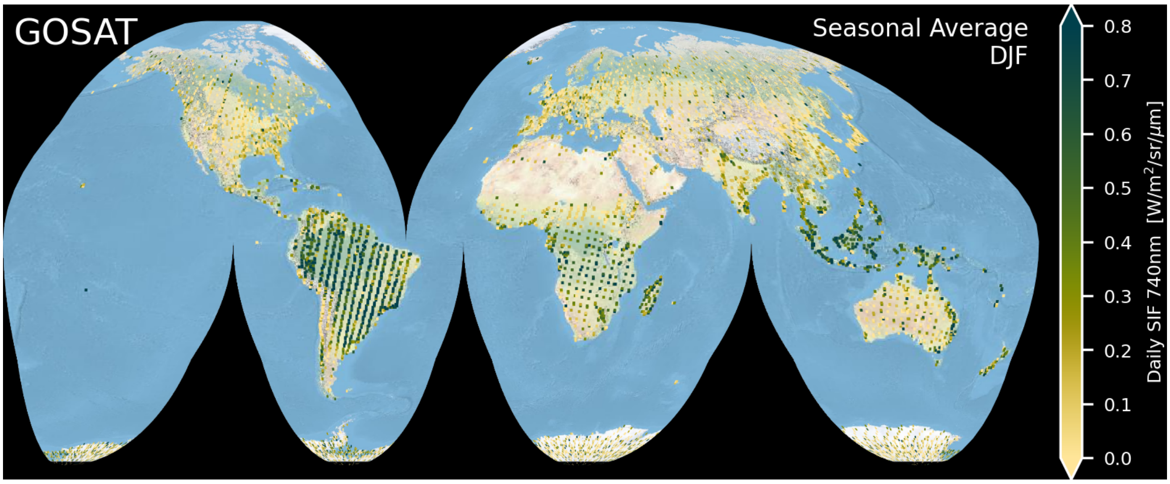

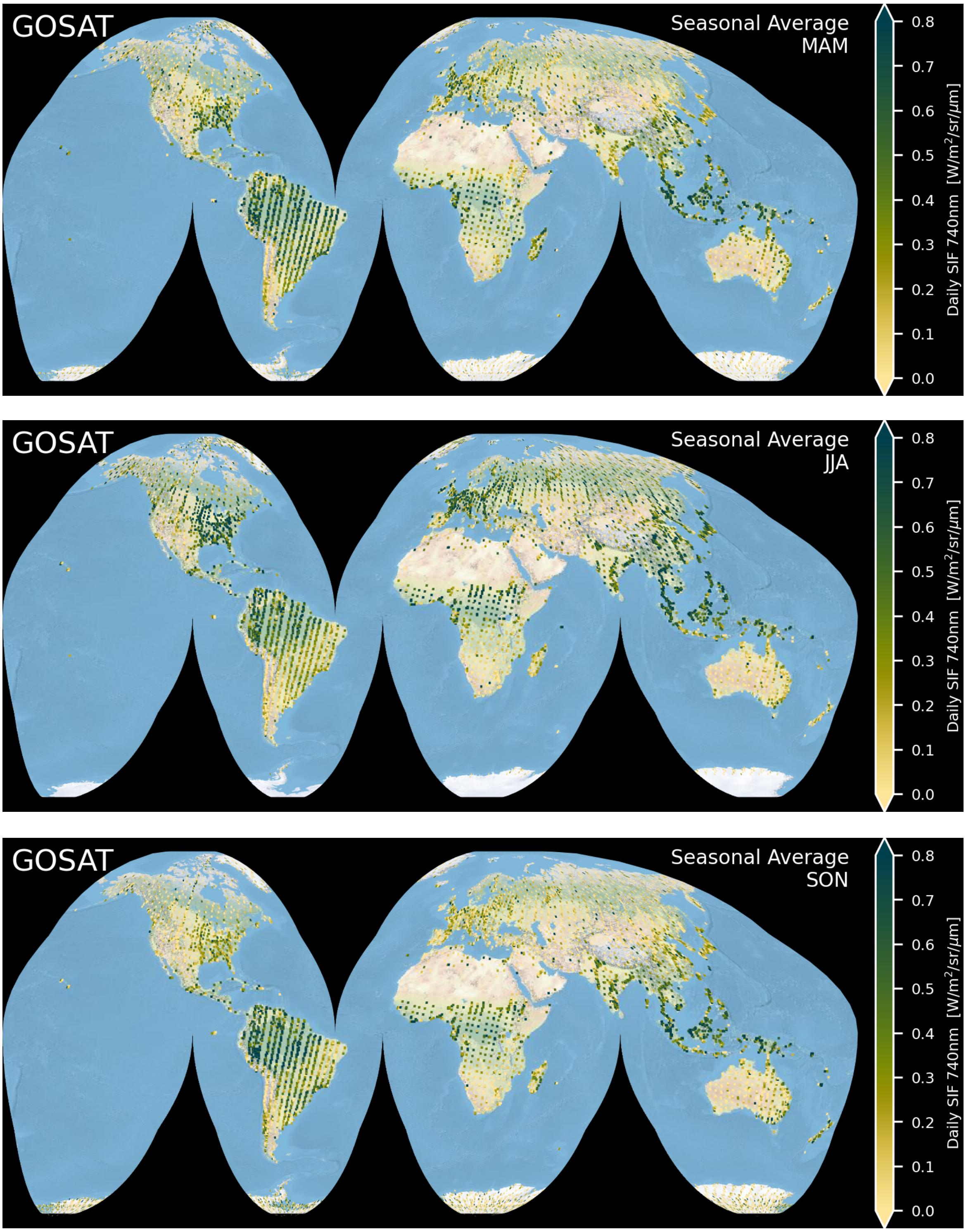
GOSAT
Seasonal Average
MAM
Daily SIF 740nm [W/m²/sr/μm]
0.0
0.1
0.2
0.3
0.4
0.5
0.6
0.7
0.8
GOSAT
Seasonal Average
JJA
Daily SIF 740nm [W/m²/sr/μm]
GOSAT
Seasonal Average
SON
Daily SIF 740nm [W/m²/sr/μm]

GLOBAL IMAGES

The revolving images on the right show monthly averages of Solar Induced Fluorescence at 740 nm, alternating between OCO-2 and OCO-3 for the period of 09/2019 through 09/2020 (excluding OCO-3 for 11/2019 due to the sparse data coverage caused by prolonged periods of non-operation of the instrument). Data have been limited to quality flags 0 (best) and 1 (good) and gridded to 0.2°×0.2°.

Note the difference in spatial coverage between OCO-2 (global) and OCO-3 (limited to a band between ±52° latitude). Also note the difference in spatial coverage from month to month in OCO-3 observations, a result of the precessing orbit of the ISS, which dictates when and where OCO-3 is in the sunlit part of the Earth. Finally, note the difference in OCO-3 spatial coverage between 09/2019 and 09/2020 (see images below): within the past year, the ISS has adjusted its orbit to a slightly higher altitude, which results in less precession of the ground track, obvious in the more regular diamond pattern over *e.g.*, Africa and South America: at the new orbital altitude, the spatial displacement between consecutive overpasses is smaller, substantially reducing the spatial drift over the course of a month.

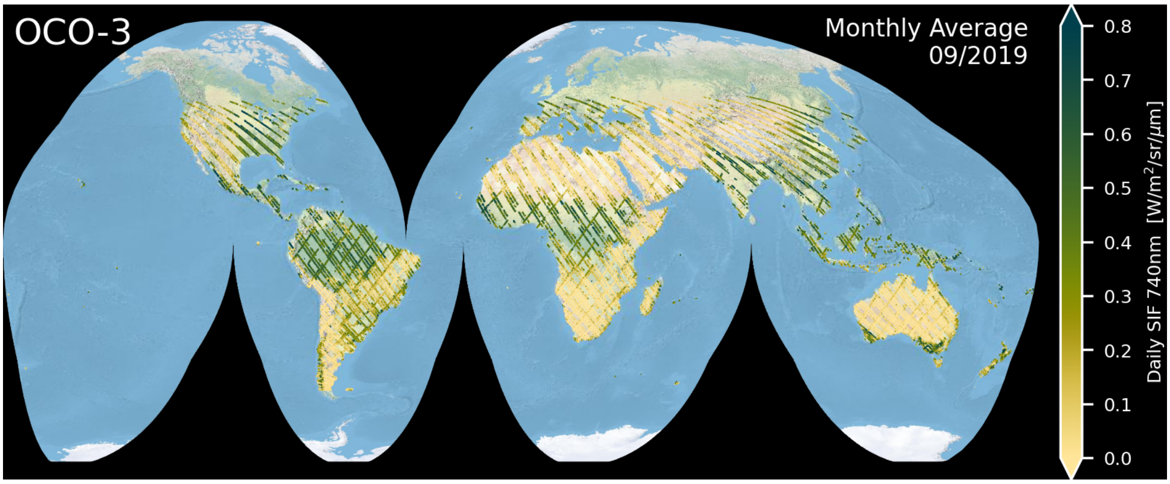

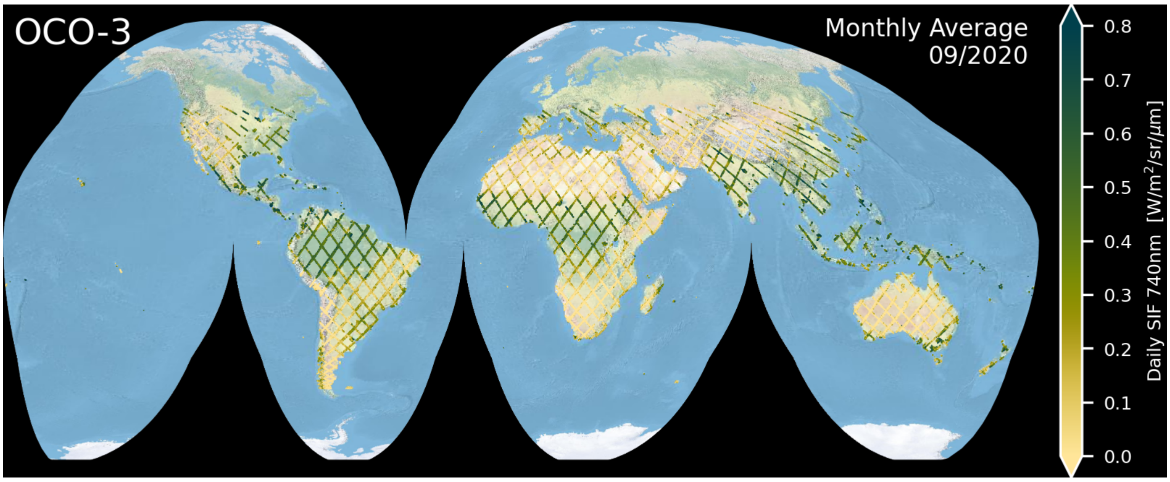

DATA PRODUCT FILE ACCESS AND VISUALIZATION

The data format of the OCO-2&3 B10 SIF Lite product is netCDF4, which is understood easily enough by most programming languages (Python, IDL, Matlab, *etc*.). To facilitate data access and visualization, a small set of in Python3-based scripts are currently being developed. If you are interested in any of the tools listed below, please contact

thomas.kurosu@jpl.nasa.gov

Data Reader – netCDF4-based

This script reads – either completely or partially – any netCDF4 file recursively and returns the contents, including all attributes, dimensions, groups, and variables (with their attributes). The returned data dictionary can be organized to either mirror the file structure (groups, variables within groups, *etc*.) or “flat”. This code is completed and available on request.

Data Reader – HDF5-based

This scripts reads – either completely or partially – any HDF5 or netCDF4 file recursively and returns the values of the data fields in a “flat” data dictionary. This code is completed and available on request.

OCO-3 Sequencer/ Segmenting Tool

Outside the OCO-3 Level-1b product, which contains the full set of observations, it can be difficult to reconstruct special observation modes – in particular Target and SAM – because only successfully retrieved soundings are included in higher-level products, and the sounding record is not necessarily contiguous. Given that, at present, information on which Target/SAM location was observed is not included in the OCO-3 product files, reconstructing which sounding was taken over what Target/SAM is not straight forward. With this in mind, a Sequencer/ Segmenting tool is being developed that combines L1b data with the list of successfully observed Targets and SAMs, to collate information on name, start and end points of observation time and sounding IDs, as well as latitude and longitude range for the full sequence as well as individual segments (“data stripes”) within the sequences. This code is mostly developed, and sample output is available on request.

OCO-3 Sequence and Segment Plotting Tool

The output from the OCO-3 Sequencer/Segmenting tool facilitates a simpler approach to data visualization of SAM and Target observations from any data product, since the boundaries of both the sequences and their segments are known (observation time stamp and footprint sounding id are present in all data products). The aim of this plotting tool is to be as generic and flexible as possible, in order to work with L1b, L2, and Lite product data fields. A β-version of this tool has been completed, with development of a more user-friendly code still on-going.

REFERENCES

Frankenberg, C., Butz, A., & Toon, G. C. (2011a). Disentangling chlorophyll fluorescence from atmospheric scattering effects in O_2 A-band spectra of reflected sun-light. Geophysical Research Letters, 38, L03801.

Frankenberg, C., Fisher, J., Worden, J., Badgley, G., Saatchi, S., Lee, J.-E., *et al*. (2011b). New global observations of the terrestrial carbon cycle from GOSAT: Patterns of plant fluorescence with gross primary productivity. Geophysical Research Letters, 38(17), L17706.

Frankenberg, C., O'Dell, C., Guanter, L., & McDuffie, J. (2012). Remote sensing of near-infrared chlorophyll fluorescence from space in scattering atmospheres: implications for its retrieval and interferences with atmospheric CO2 retrievals. Atmospheric Measurement Techniques, 5(8), 20812094.

Frankenberg, C., O'Dell, C., Berry, J., Guanter, L., Joiner, J., Köhler, P., *et al*. (2014). Prospects for chlorophyll fluorescence remote sensing from the Orbiting Carbon Observatory-2. Remote Sensing of Environment, 147(0), 112.

Guanter, L., Rossini, M., Colombo, R., Meroni, M., Frankenberg, C., Lee, J.-E., & Joiner, J. (2013). Using field spectroscopy to assess the potential of statistical approaches for the retrieval of sun-induced chlorophyll fluorescence from ground and space. Remote Sensing of Environment, 133(0), 5261.

Guanter, L., Frankenberg, C., Dudhia, A., Lewis, P. E., Gómez-Dans, J., Kuze, A., *et al*. (2012). Retrieval and global assessment of terrestrial chlorophyll fluorescence from GOSAT space measurements. Remote Sensing of Environment, 121, 236251.

Joiner, J., Guanter, L., Lindstrot, R., Voigt, M., Vasilkov, A. P., Middleton, E. M., *et al*. (2013). Global monitoring of terrestrial chlorophyll fluorescence from moderate spectral resolution near-infrared satellite measurements: Methodology, simulations, and application to GOME-2. Atmospheric Measurement Techniques Discussions, 6(2), 3883–3930. https://doi.org/10.5194/amtd-6-3883-2013.

Köhler, P., Guanter, L., Kobayashi, H., Walther, S., & Yang, W. (2018). Assessing the potential of Sun-induced fluorescence and the canopy scattering coefficient to track large-scale vegetation dynamics in Amazon forests. Remote Sensing of Environment, 204, 769–785. https:// doi.org/10.1016/j.rse.2017.09.025

Lee, J.-E., Frankenberg, C., van der Tol, C., Berry, J. A., Guanter, L., Boyce, C. K., *et al*. (2013). Forest productivity and water stress in Amazonia: observations from GOSAT chlorophyll fluorescence. Proceedings of the Royal Society B: Biological Sciences, 280(1761).

Magney, T. S., Frankenberg, C., Köhler, P., North, G., Davis, T. S., Dold, C., *et al*. (2019). Disentangling changes in the spectral shape of chlorophyll fluorescence: implications for remote sensing of photosynthesis. Journal of Geophysical Research: Biogeosciences, 124, 1491–1507. https://doi.org/10.1029/2019JG005029

Parazoo, N.C., C. Frankenberg, P. Köhler, J. Joiner, Y. Yoshida, T. Magney, Y. Sun, V. Yadav, Towards a harmonized long-term spaceborne record of far-red solar induced fluorescence, 2019: JGR-Biogeosciences, 124 (8), 2518-2539.

Sun, Y., Frankenberg, C., Jung, M., Joiner, J., Guanter, L., Köhler, P., & Magney, T. (2018). Overview of solar-induced chlorophyll fluorescence (SIF) from the Orbiting Carbon Observatory-2: Retrieval, cross-mission comparison, and global monitoring for GPP. Remote Sensing of Environment, 209(February), 808–823. https://doi.org/10.1016/j.rse.2018.02.016

Zhang, Y., Xiao, X., Wu, X. *et al*. A global moderate resolution dataset of gross primary production of vegetation for 2000–2016. Sci Data 4, 170165 (2017). https://doi.org/10.1038/sdata.2017.165.